ISSN 2347-3487

PARTICLE-HOLE PAIR AND BEELECTRON STATES IN ZnO/(Zn,Mg)O QUANTUM WELLS AND DIRAC MATERIALS.

Lyubov E. Lokot
Institute of Semiconductor Physics, NAS of Ukraine, 41, Nauky Ave., Kyiv 03028, Ukraine

ABSTRACT

In this paper a theoretical studies of the space separation of electron and hole wave functions in the quantum well $ZnO/Mg_{0.27}Zn_{0.73}O$ are presented. For this aim the self-consistent solution of the Schrödinger equations for electrons and holes and the Poisson equations at the presence of spatially varying quantum well potential due to the piezoelectric effect and local exchange-correlation potential is found. The one-dimensional Poisson equation contains the Hartree potential which includes the one-dimensional charge density for electrons and holes along the polarization field distribution. The three-dimensional Poisson equation contains besides the one-dimensional charge density for electrons and holes the exchange-correlation potential which is built on convolutions of a plane-wave part of wave functions in addition. The shifts of the Hartree valence band spectrums and the conduction band spectrum with respect to the flat band spectrums as well as the Hartree-Fock band spectrums with respect to the Hartree ones are found. An overlap integrals of the wave functions of holes and electron with taking into account besides the piezoelectric effects the exchange-correlation effects in addition is greater than an overlap integral of Hartree ones. The Hartree particles distribute greater on edges of quantum well than Hartree-Fock particles. It is found that an effective mass of heavy hole of $Mg_{0.27}Zn_{0.73}O$ under biaxial strain is greater than an effective-mass of heavy hole of ZnO. It is calculated that an electron mass is less than a hole mass. It is found that the Bohr radius is grater than the localization range particle-hole pair, and the excitons may be spontaneously created.

Schrödinger equation for pair of two massless Dirac particles when magnetic field is applied in Landau gauge is solved exactly. In this case the separation of center of mass and relative motion is obtained. Landau quantization $\varepsilon = \pm B\sqrt{l}$ for pair of two Majorana fermions coupled via a Coulomb potential from massless chiral Dirac equation in cylindric coordinate is found. The root ambiguity in energy spectrum leads into Landau quantization for beelectron, when the states in which the one simultaneously exists are allowed. The tachyon solution with imaginary energy in Cooper problem ($\varepsilon^2 < 0$) is found.

Indexing terms/Keywords

Particle-hole pair; beelectron; quantum well; grapheme; Dirac cone; tachyon.

Introduction

There has been widely studied in the ultraviolet spectral range lasers based on direct wide-bandgap hexagonal würtzite crystal material systems such as ZnO [1-6]. Significant success has been obtained in growth ZnO quantum wells with (ZnMg)O barriers by scrutinized methods of growth [7,8]. The carrier relaxation from (ZnMg)O barrier layers into a ZnO quantum well through time-resolved photoluminescense spectroscopy is studied in the paper [9]. The time of filling of particles for the single ZnO quantum well is found to be 3 ps [9].

In the paper we present a theoretical investigation of the intricate interaction of the electron-hole plasma with a polarization-induced electric fields. The confinement of wave functions has a strong influence on the optical properties which is observed with a dependence from the intrinsic electric field which is calculated to be 0.37 MV/cm [10], causing to the quantum-confined Stark effect (QCSE). In this paper we present the results of theoretical studies of the space separation of electron and hole wave functions by self-consistent solution of the Schrödinger equations for electrons and holes and the Poisson equations at the presence of spatially varying quantum well potential due to the piezoelectric effect and the local exchange-correlation potential.

In addition large electron and hole effective masses, large carrier densities in quantum well ZnO are of cause for population inversions. These features are comparable to GaN based systems [11,12].

A variational simulation in effective-mass approximation is used for the conduction band dispersion and for quantization of holes a Schrödinger equation is solved with würtzite hexagonal effective Hamiltonian [13] including deformation potentials [14]. Keeping in mind the above mentioned equations and the potential energies which have been included in this problem from Poisson's equations we have obtained completely self-consistent band structures and wave functions.

So in this paper we present a self-consistent calculation an above mentioned equations in würtzite ZnO quantum well taking into account the piezoelectric effect and the exchange-correlation potential for bandgap renormalization and engineering of localized Hartree-Fock wave functions. The energy shifts as well as the localization range of exchange-correlational wave functions with respect to Hartree energy shifts and Hartree localization range of wave functions require a scrutiny study.

We consider the pairing between oppositely charged particles with complex dispersion. The Coulomb interaction leads to the electron-hole bound states scrutiny study of which acquire significant attention in the explanations of superconductivity. If the exciton binding energy is grater than the localization range particle-hole pair, the excitons may be spontaneously created.

2 Theoretical study

A. Effective Hamiltonian

It is known [13,15] that the valence-band spectrum of hexagonal würtzite crystal at the Γ point originates from the sixfold degenerate Γ_{15} state. Under the action of the hexagonal crystal field in würtzite crystals, Γ_{15} splits and leads to the formation of two levels: Γ_1, Γ_5. The wave functions of the valence band transform according to the representation $\Gamma_1+\Gamma_5$ of the point group C_{6v}, while the wave function of the conduction band transforms according to the representation Γ_1.

C_{6v}	E	C_2	$2C_3$	$2C_6$	$3\sigma_v$	$3\sigma_v'$	
$\Gamma_1+\Gamma_5$	3	-1	0	2	1	1	
g^2	E	E	C_3	C_3	E	E	
$\chi_\psi^2(g)$	9	1	0	4	1	1	
$\chi_\psi(g^2)$	3	3	0	0	3	3	
$\frac{1}{2}[\chi_\psi^2(g)+\chi_\psi(g^2)]$	6	2	0	2	2	2	$2\Gamma_1+\Gamma_5+\Gamma_6$
$\frac{1}{2}\{\chi_\psi^2(g)-\chi_\psi(g^2)\}$	3	-1	0	2	-1	-1	$\Gamma_2+\Gamma_5$

ISSN 2347-3487

An irreducible presentations for orbital angular momentum j may be built from formula

$$\chi_j(\varphi) = \frac{\sin(j+\frac{1}{2})\varphi}{\sin\frac{\varphi}{2}}. \quad (1)$$

For the vector representational $j=1$

$$\chi_v(\varphi) = \frac{\sin\frac{3\varphi}{2}}{\sin\frac{\varphi}{2}} = 1 + 2\cos\varphi. \quad (2)$$

C_{6v}	E	C_2	$2C_3$	$2C_6$	$3\sigma_v$	$3\sigma_v'$	
χ_v	3	-1	0	2	1	1	$\Gamma_1+\Gamma_5$
$\frac{1}{2}[\chi_v^2(g)+\chi_v(g^2)]$	6	2	0	2	2	2	$2\Gamma_1+\Gamma_5+\Gamma_6$
$\frac{1}{2}\{\chi_v^2(g)-\chi_v(g^2)\}$	3	-1	0	2	-1	-1	$\Gamma_2+\Gamma_5$

The direct production of two irreducible presentations of wave function and wave vector of difference $\kappa-\Gamma$ expansion with taken into account time inversion can be expanded on

$$\begin{aligned} p^\alpha : \tau_v \times \tau_\psi &= (\Gamma_1+\Gamma_5)\times(\Gamma_2+\Gamma_5) = \\ &= \Gamma_5\times\Gamma_5, \end{aligned} \quad (3)$$

for the square of wave vector

$$\begin{aligned} [p^\alpha p^\beta] : \tau_{v^2} \times \tau_\psi &= (2\Gamma_1+\Gamma_5+\Gamma_6)\times(2\Gamma_1+\Gamma_5+\Gamma_6) = \\ &= 4\Gamma_1\times\Gamma_1+\Gamma_5\times\Gamma_5+\Gamma_6\times\Gamma_6. \end{aligned} \quad (4)$$

In the low-energy limit the Hamiltonian of würtzite

$$\begin{aligned} \hat{H}_0 &= I(\Delta_1+\Delta_2)+ \\ &+\Delta_1 J_z^2+\Delta_2 J_z\sigma_z+\sqrt{2}\Delta_3(J_+\sigma_-+J_-\sigma_+), \end{aligned} \quad (5)$$

$$\begin{aligned} \hat{H}_k &= A_1k_z^2+A_2k_t^2+(A_3k_z^2+A_4k_t^2)J_z^2+ \\ &+A_5k_z(2[J_zJ_+]k_-+2[J_zJ_-]k_+)+ \\ &+A_6(J_+^2k_-^2+J_-^2k_+^2)+iA_7(J_+k_--J_-k_+), \end{aligned} \quad (6)$$

$$\begin{aligned} \hat{H}_\varepsilon &= D_1\varepsilon_{zz}+D_2\varepsilon_\perp^2+(D_3\varepsilon_{zz}+D_4\varepsilon_\perp)J_z^2+ \\ &+D_5(2[J_zJ_+]\varepsilon_{-z}+2[J_zJ_-]\varepsilon_{+z})+ \\ &+D_6(J_+^2\varepsilon_-+J_-^2\varepsilon_+). \end{aligned} \quad (7)$$

In the basis of spherical wave functions with the orbital angular momentum $l=1$ and the eigenvalue m_l of its z component:

$$
\begin{aligned}
|1,\varsigma_v\rangle &= \frac{1}{\sqrt{2}}(Y_1^1\psi(1/2)e^{-3i\varphi/2}e^{-3i\pi/4} \pm Y_1^{-1}\psi(-1/2)e^{3i\varphi/2}e^{3i\pi/4}) \\
|2,\varsigma_v\rangle &= \frac{1}{\sqrt{2}}(\pm Y_1^1\psi(-1/2)e^{-i\varphi/2}e^{-i\pi/4} + Y_1^{-1}\psi(1/2)e^{i\varphi/2}e^{i\pi/4}) \\
|3,\varsigma_v\rangle &= \frac{1}{\sqrt{2}}(\pm Y_1^0\psi(1/2)e^{-i\varphi/2}e^{-i\pi/4} + Y_1^0\psi(-1/2)e^{i\varphi/2}e^{i\pi/4})
\end{aligned}, \tag{8}
$$

the Hamiltonian may be transformed to the diagonal form indicating two spin degeneracy [18]:

$$
H_\pm = \begin{Vmatrix} F & K_t & \mp iH_t \\ K_t & G & \Delta \mp iH_t \\ \pm iH_t & \Delta \pm iH_t & \lambda \end{Vmatrix} \begin{matrix} |1,\varsigma_v\rangle \\ |2,\varsigma_v\rangle, \\ |3,\varsigma_v\rangle \end{matrix} \tag{9}
$$

where $F = \Delta_1 + \Delta_2 + \lambda + \theta$, $G = \Delta_1 - \Delta_2 + \lambda + \theta$, $\lambda = \lambda_k + \lambda_\varepsilon$, $\theta = \theta_k + \theta_\varepsilon$, $\lambda_k = \frac{\hbar^2}{2m_0}(A_1k_z^2 + A_2k_t^2)$, $\lambda_\varepsilon = D_1\varepsilon_{zz} + D_2(\varepsilon_{xx} + \varepsilon_{yy})$, $\theta_k = \frac{\hbar^2}{2m_0}(A_3k_z^2 + A_4k_t^2)$, $\theta_\varepsilon = D_3\varepsilon_{zz} + D_4(\varepsilon_{xx} + \varepsilon_{yy})$, $K_t = \frac{\hbar^2}{2m_0}(A_5k_t^2)$, $H_t = \frac{\hbar^2}{2m_0}(A_6k_tk_z)$, $\Delta = \sqrt{2}\Delta_3$, $k_t^2 = k_x^2 + k_y^2$.

From Kane model one can define the band-edge parameters such as the crystal-field splitting energy Δ_{cr}, the spin-orbit splitting energy Δ_{so} and the momentum-matrix elements for the longitudinal ($e\|z$) z-polarization and the transverse ($e \perp z$) polarization : $P_z \equiv \langle S|\hat{p}_z|Z\rangle$, $P_\perp \equiv \langle S|\hat{p}_x|X\rangle \equiv \langle S|\hat{p}_y|Y\rangle$. Here we use the effective-mass parameters, energy splitting parameters, deformation potential parameters as in papers [14,16,17].

We consider a quantum well of width w in ZnO under biaxial strain, which is oriented perpendicularly to the growth direction (0001) and localized in the spatial region $-w/2 < z < w/2$. In the ZnO/MgZnO quantum well structure, there is a strain-induced electric field. This piezoelectric field, which is perpendicular to the quantum well plane (i.e., in z direction) may be appreciable because of the large piezoelectric constants in würtzite structures.

The transverse components of the biaxial strain are proportional to the difference between the lattice constants of materials of the well and the barrier and depend on the Mg content x: $\varepsilon_{xx} = \varepsilon_{yy} = \frac{a_{Mg_xZn_{1-x}O} - a_{ZnO}}{a_{ZnO}}$, $a_{Mg_xZn_{1-x}O} = a_{ZnO} + x(a_{MgO} - a_{ZnO})$, $a_{ZnO} = 0.32496$ nm, $a_{MgO} = 0.4216$ nm [17]. The longitudinal component of a deformation is expressed through elastic constants and the transverse component of a deformation: $\varepsilon_{zz} = -2\frac{C_{13}}{C_{33}}\varepsilon_{xx}$.

The physical parameters for ZnO are as follows. We take the effective-mass parameters [16]: $A_1 = -2.743$, $A_2 = -0.393$, $A_3 = 2.377$, $A_4 = -2.069$, $A_5 = -2.051$, $A_6 = -2.099$, $m_e^{z,\perp} = 0.329m_0$, where m_0 is the electron rest mass in the vacuum, the parameters for deformation potential [14]: $D_1 = -3800$ meV, $D_2 = -3800$ meV, $D_3 = -800$ meV, $D_4 = 1400$ meV, $D_{cz} := -6860$ meV, $D_{c\perp} := -6260$ meV, and the energy parameters at 300 K [16,17]: $E_g = 3400$ meV, $\Delta_1 = \Delta_{cr} = 36.3$ meV, $\Delta_2/3 = 0.63$ meV, $\Delta_3/3 = 2.47$ meV, $\Delta_2 = \Delta_3 = \Delta_{so}$ the elastic constant [17]: $C_{13} = 90$ GPa and $C_{33} = 196$ GPa, the permittivity of the host materials $\kappa = 7.8$.

3 ZnO/(Zn,Mg)O quantum well

We take the following wave functions written as vectors in the three-dimensional Bloch space:

$$|\nu\varsigma_\nu k_t\rangle = \left\| \begin{matrix} \sum_{i=1}^{m}\Psi_{k_t}^{(1)}[i,\nu]\psi_i(Z) \\ \sum_{i=1}^{m}\Psi_{k_t}^{(2)}[i,\nu]\psi_i(Z) \\ \sum_{i=1}^{m}\Psi_{k_t}^{(3)}[i,\nu]\psi_i(Z) \end{matrix} \right\| \begin{matrix} |1,\varsigma_\nu\rangle \\ |2,\varsigma_\nu\rangle. \\ |3,\varsigma_\nu\rangle \end{matrix} \tag{10}$$

The Bloch vector of ν-type hole with spin $\varsigma_\nu = \pm 1/2$ and momentum k_t is specified by its three coordinates $[\Psi_{k_t}^{(1)}[m,\nu], \Psi_{k_t}^{(2)}[m,\nu], \Psi_{k_t}^{(3)}[m,\nu]]$ in the basis $[|1,\varsigma_\nu\rangle, |2,\varsigma_\nu\rangle, |3,\varsigma_\nu\rangle]$ [18], known as spherical harmonics with the orbital angular momentum $l = 1$ and the eigenvalue m_l its z component. The envelope Z-dependent part of the quantum well eigenfunctions can be specified from the boundary conditions $\psi_m(Z=0) = \psi_m(Z=1) = 0$ of the infinite quantum well as

$$\psi_m(Z) = \sqrt{\frac{2}{w}}\sin(\pi m Z), \tag{11}$$

where $Z = (\frac{z}{w} + \frac{1}{2})$, m is a natural number. Thus the hole wave function can be written as

$$\Psi_{\nu\varsigma_\nu k_t}(r) = \frac{e^{ik_t\rho_t}}{\sqrt{A}}|\nu\varsigma_\nu k_t\rangle. \tag{12}$$

The valence subband structure $E_\nu^{\varsigma_\nu}(k_t)$ can be determined by solving equations system:

$$\sum_{j=1}^{3}(H_{ij}^{\varsigma_\nu}(k_z = -i\frac{\partial}{\partial z}) + V(z) + \delta_{ij}E_\nu^{\varsigma_\nu}(k_t)) \times \\ \times \phi_\nu^{(j)\varsigma_\nu}(z,k_t) = 0, \tag{13}$$

where $\phi_\nu^{(j)\varsigma_\nu}(z,k_t) = \sum_{n=1}^{m}\Psi_{k_t}^{(j)}[n,\nu]\psi_n(z)$, $i = 1,2,3$.

The wave function of electron of first energy level with accounts QCSE [19]:

$$\Psi(r) = \frac{1}{\sqrt{A}}e^{ik_t\rho}\Psi(Z,\xi)|S\rangle|\varsigma_c\rangle, \tag{14}$$

where

$$\Psi(Z,\xi) = \begin{cases} \psi_1(Z,\xi) = C_1 e^{(\kappa_0-\xi)(wZ)}, Z \in (-\infty..0) \\ \psi(Z,\xi) = C\sin(k_0 w(Z-\frac{1}{2}) + \delta_0)e^{-\xi w(Z-\frac{1}{2})}, Z \in [0..1] \\ \psi_2(Z,\xi) = C_2 e^{-(\kappa_0+\xi)w(Z-1)}, Z \in (1..\infty), \end{cases} \tag{15}$$

$|S\rangle = Y_0^0$, $\varsigma_c = \pm 1/2$.

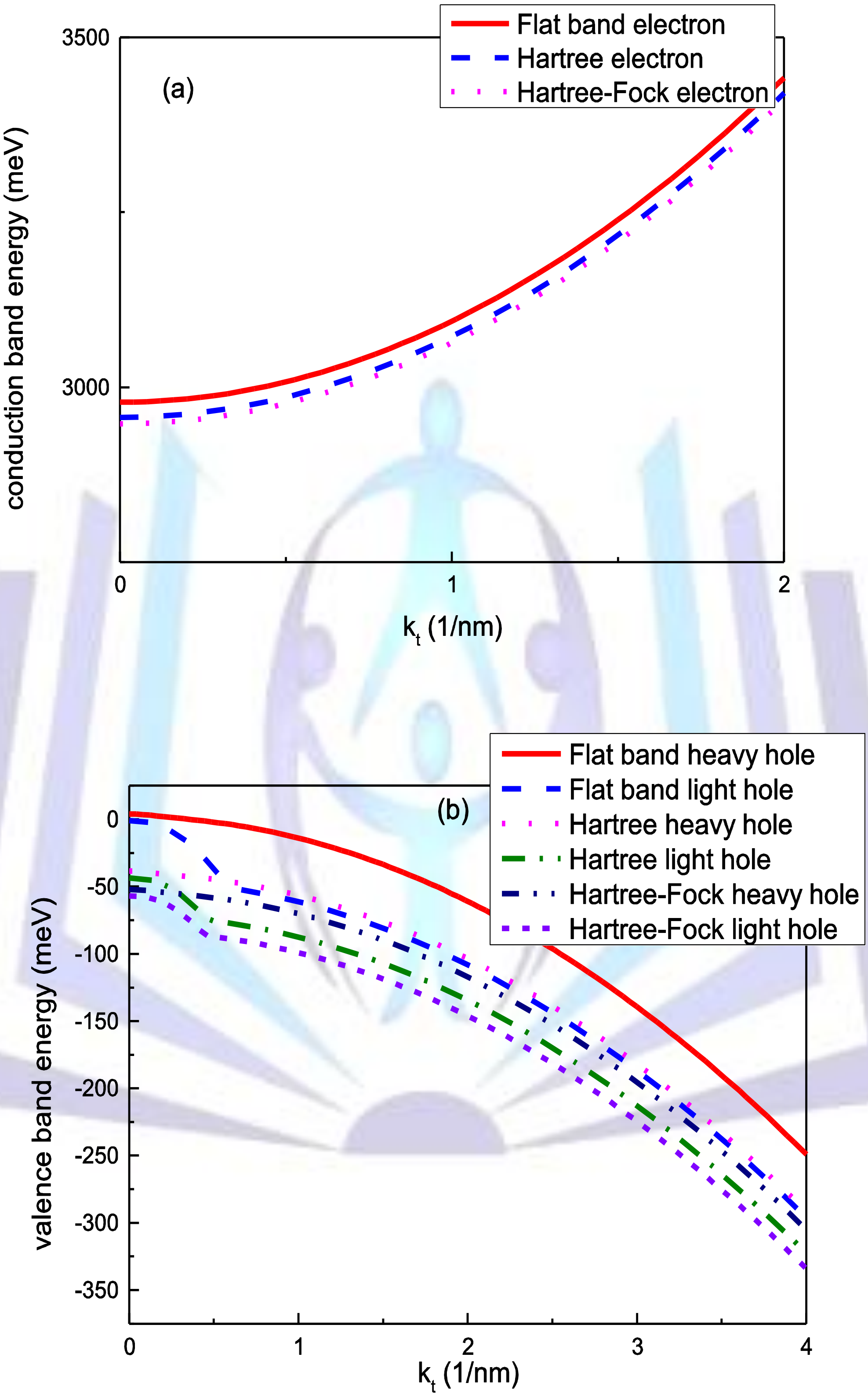

Figure 1: (Color online) For the quantum well $ZnO/Mg_{0.27}Zn_{0.73}O$ with a width 4 nm, at a carriers concentration $4*10^{12}$ cm $^{-2}$, at a temperature 300 K: (a) conduction band energy; (b) valence band energy.

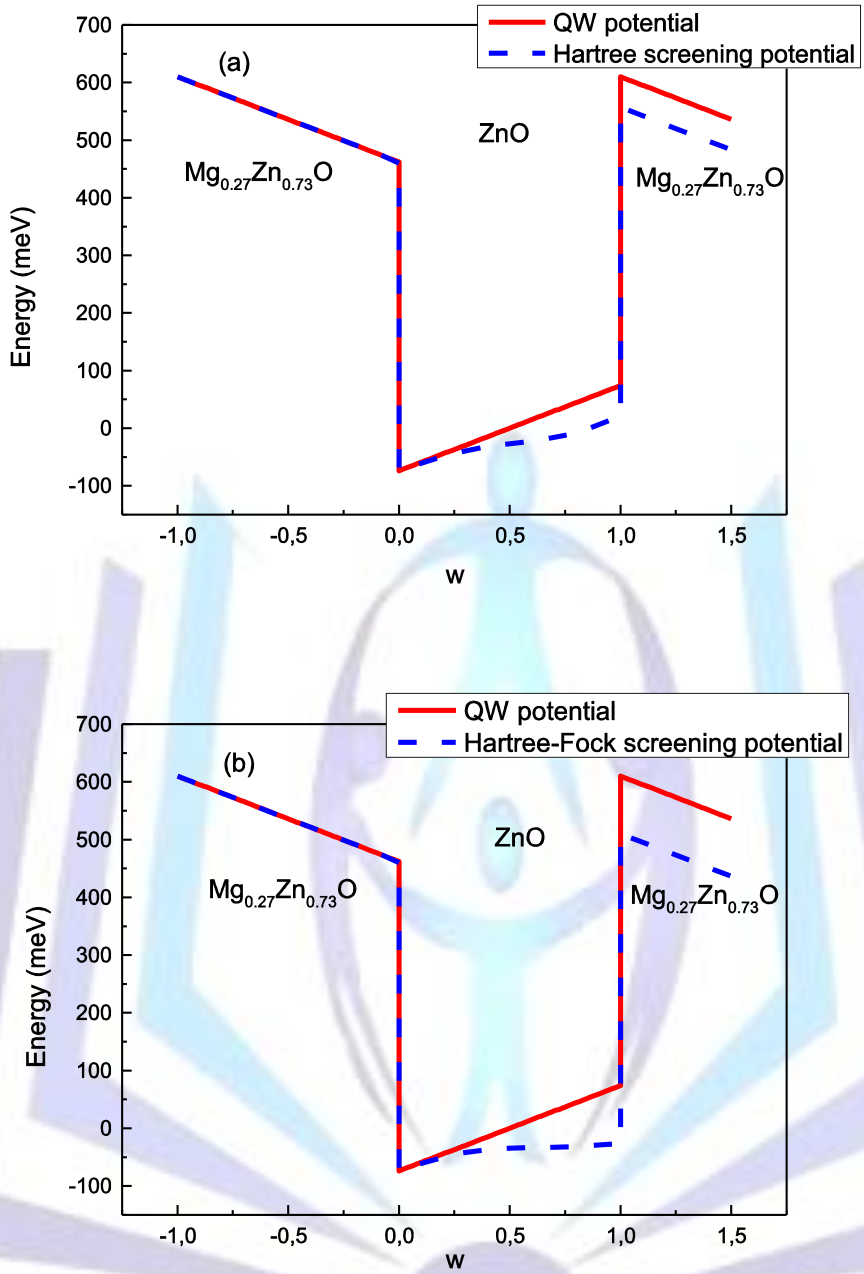

Figure 2: (Color online) For the quantum well $ZnO/Mg_{0.27}Zn_{0.73}O$ with a width 4 nm, at a carriers concentration $4*10^{12}$ cm $^{-2}$, at a temperature 300 K: (a) Hartree screening potential; (b) Hartree-Fock screening potential.

From bond conditions [19,20] $\psi_1(Z,\xi)|_{Z=0}=\psi(Z,\xi)|_{Z=0}$, $\psi_2(Z,\xi)|_{Z=1}=\psi(Z,\xi)|_{Z=1}$, $\frac{\psi_1'(Z,\xi)}{\psi_1(Z,\xi)}|_{Z=0}=\frac{\psi'(Z,\xi)}{\psi(Z,\xi)}|_{Z=0}$, $\frac{\psi_2'(Z,\xi)}{\psi_2(Z,\xi)}|_{Z=1}=\frac{\psi'(Z,\xi)}{\psi(Z,\xi)}|_{Z=1}$, one can find $C_1 = C\sin(-\frac{k_0 w}{2}+\delta_0)e^{\xi\frac{w}{2}}$, $C_2 = C\sin(\frac{k_0 w}{2}+\delta_0)e^{-\xi\frac{w}{2}}$, $\kappa_0 = k_0(\frac{1-\cos k_0 w}{\sin k_0 w})$, $\delta_0 = \frac{k_0 w}{2}+\arctan\frac{\kappa_0}{k_0}$, where A is the area of the quantum well in the xy plane, ρ is the two-dimensional vector in the xy plane, $k_t=(k_x,k_y)$ is in-plane wave vector. The constant multiplier C is found from normalization condition:

$$\int_{-\infty}^{\infty} |\Psi(Z,\xi)|^2 \; wdZ = 1. \tag{16}$$

One can find the functional, which is built in the form:

$$J(\xi) = \frac{\langle \Psi | \hat{H} | \Psi \rangle}{\langle \Psi | \Psi \rangle}, \tag{17}$$

where

$$H = H_c + V(z), \tag{18}$$

where H_c is a conduction band kinetic energy including deformation potential:

$$\begin{aligned} H_c = E_g + \Delta_1 + \Delta_2 + \frac{\hbar^2}{2m_e^{\perp}} k_t^2 - \frac{\hbar^2}{2m_e^z} \frac{\partial^2}{\partial z^2} + \\ + D_{cz}\varepsilon_{zz} + D_{c\perp}(\varepsilon_{xx} + \varepsilon_{yy}). \end{aligned} \tag{19}$$

The potential energies $V(z)$ can look for as follows:

$$V(z) = e\Phi^H(z) + \delta U_{c,v}(z) + \Phi_{xc}(z), \tag{20}$$

where $\Phi^H(z)$ is the solution of one-dimensional Poisson's equation with the strain-induced electric field in the quantum well, $\delta U_{c,v}(z)$ are the conduction and valence bandedge discontinuities which can be represented in the form [21]:

$$\delta U_c(z) = \begin{cases} U_0 - eEw(\frac{z}{w}+1), z \in (-\infty..-w/2) \\ eEz, z \in [-w/2..w/2] \\ U_0 - eEw(\frac{z}{w}-1), z \in (w/2..\infty). \end{cases} \tag{21}$$

$\Phi_{xc}(z)$ is exchange-correlation potential energy which is found from the solution of three-dimensional Poisson's equation, using both an expression by Gunnarsson and Lundquist [22], and following criterions. At carrier densities $4*10^{12}$ cm $^{-2}$, the criterion $k_F > \sqrt{n}/4$ at a temperature T=0 K as $1 > 0.1$ has been carried. k_F is Fermi wave vector. The criterion does not depend from a width of well. The ratio of Coulomb potential energy to the Fermi energy is $r_s = E_C/E_F = 0.63 < 1$. The problem consists of the one-dimensional Poisson's equation solving of which may be found Hartree potential energy and three-dimensional Poisson's equation which is separated on one-dimensional and two-dimensional equations by separated of variables using a criterion $[\Psi_{\alpha,\nu,n}(k_F, z)\sin \mathbf{k}_F \boldsymbol{\rho}] << 1$, where $\alpha = e,h$. The three-dimensional Poisson's equation includes local exchange-correlation potential:

$$\frac{d^2\Phi_{e,h}}{dz^2} + \Delta_\rho \Phi_{e,h} = \frac{4\pi}{\kappa}(\rho_{e,h}^H(z;g) + \rho_{e,h}^{xc}(\mathbf{r},\mathbf{r}')), \tag{22}$$

$$\frac{d^2\Phi_{e,h}^H}{dz^2} = \frac{4\pi}{\kappa}\rho_{e,h}^H(z;g), \tag{23}$$

$$\Delta_\rho \Phi_{e,h}^{xc} = \frac{4\pi}{\kappa}\rho_{e,h}^{xc}(\mathbf{r},\mathbf{r}'), \tag{24}$$

where

$$\rho_{e,h}^H(z;g) = \mp e \sum_{\nu,n,k_t} |\Psi_{e,h,\nu,n}(k_t,z)|^2 \; f_{n,\nu}(k_t;g), \tag{25}$$

$$f_{n,\nu}(k_t;g)=\frac{1}{e^{(\varepsilon_{n,\nu,k_t}+\frac{g}{2}\sum\limits_{i\neq j}\frac{1}{|\mathbf{r}_i-\mathbf{r}_j|}-\mu)/kT}+1}= \\ =\frac{1}{(e^1(1+r_s+r_s^2+...))^{(\varepsilon_{n,\nu,k_t}-\mu)/kT}+1}. \tag{26}$$

The solution of equations system (13), (17), (22) as well as (13), (17), (23) does not depend from a temperature.

Solving one-dimensional Poisson's equation (23) one can find screening polarization field and Hartree potential energy by substituting her in the Schrödinger equations. From Schrödinger equations wave functions and bandstructure are found. The conclusive determination of screening polarization field is determined by iterating Eqs. (13), (17), (22) until the solutions of conduction and valence band energies and wave functions are converged:

$$\Phi^H(z)=\Phi_h^H(z)+\Phi_e^H(z), \tag{27}$$

$$e\Phi_h^H(z)=\frac{2e^2}{\kappa}\sum_{\nu,m,l,i}g_\nu\int k_t dk_t\langle\nu_i,\varsigma_\nu\,|\,\Psi_{k_t}^i[\nu,m]\Psi_{k_t}^i[\nu,l]\,|\,\varsigma_\nu,\nu_i\rangle f_{\nu,p}(k_t)\times \\ \times\begin{cases} w\left(\frac{\cos\pi(\frac{z}{w}+\frac{1}{2})(l+m)}{\pi^2(l+m)^2}-\frac{\cos\pi(\frac{z}{w}+\frac{1}{2})(m-l)}{\pi^2(m-l)^2}\right), m\neq l \\ w\left(\frac{(\frac{z}{w}+\frac{1}{2})^2}{2}+\frac{1}{4}\frac{\cos 2\pi m(\frac{z}{w}+\frac{1}{2})}{\pi^2 m^2}\right), m=l, \end{cases} \tag{28}$$

$$e\Phi_e^H(z)=-\frac{2e^2}{\kappa}g_1\int k_t dk_t C^2 f_{1n}(k_t)\times \\ \times\begin{cases} \frac{1-\cos(-k_0w+2\delta_0)}{2}e^{\xi w}\frac{e^{2(\kappa_0-\xi)(z+\frac{w}{2})}}{4(\kappa_0-\xi)^2}, z\in(-\infty..-w/2) \\ \frac{e^{-2\xi z}}{8\xi^2}-\frac{2\cos 2(k_0z+\delta_0)e^{-2\xi z}}{(4\xi^2+4k_0^2)^2}(\xi^2-k_0^2)+\frac{\sin 2(k_0z+\delta_0)e^{-2\xi z}}{4(\xi^2+k_0^2)^2}k_0\xi, z\in[-w/2..w/2] \\ \frac{1-\cos(k_0w+2\delta_0)}{2}e^{-\xi w}\frac{e^{-2(\kappa_0+\xi)(z-\frac{w}{2})}}{4(\kappa_0+\xi)^2}, z\in(w/2..\infty), \end{cases} \tag{29}$$

where $Z=\frac{z}{w}+\frac{1}{2}$, g_ν and g_1 correspond to the degeneration of the ν hole band and the first quantized conduction band, respectively, e is the value of electron charge, κ is the permittivity of a host material, and $f_{\nu,p}(k_t)$, $f_{1n}(k_t)$ are the Fermi-Dirac distributions for holes and electrons.

Exchange-correlation charge density may be determined as:

$$\rho_{e,h}^{xc}(\mathbf{r},\mathbf{r}')= \\ =\sum_{l=0}^{\infty}\sum_{m=-l}^{l}|\,\Psi_{\alpha,\nu,n}(k_t,z)|^2\;\rho_{lm}(\boldsymbol{\rho}-\boldsymbol{\rho}')Y_{lm}\left(\frac{\boldsymbol{\rho}-\boldsymbol{\rho}'}{|\boldsymbol{\rho}-\boldsymbol{\rho}'|}\right), \tag{30}$$

using the expansion of plane wave

$$\sum_{l=0}^{\infty}\sum_{m=-l}^{l}\rho_{lm}(\boldsymbol{\rho})Y_{lm}(\frac{\boldsymbol{\rho}}{|\boldsymbol{\rho}|}) = \\ = e^{ik_t\boldsymbol{\rho}} = 4\pi\sum_{l=0}^{\infty}\sum_{m=-l}^{l} i^l j_l(k_t\boldsymbol{\rho})Y^*_{lm}(\frac{k_t}{k_t})Y_{lm}(\frac{\boldsymbol{\rho}}{|\boldsymbol{\rho}|}). \tag{31}$$

At the condition $[\Psi_{\alpha,\nu,n}(k_F,z)\sin k_F\boldsymbol{\rho}] << 1$, the solution Eq. (24) may be found as follows

$$\Phi_{e,h}(xc) = \int_0^\infty \rho\rho_{00}(\boldsymbol{\rho})\frac{1}{\rho}d\rho. \tag{32}$$

The solution the three-dimensional Poisson's equation may be presented in the form:

$$\Phi^{xc}_{e,h}(z) = \Phi^H_{e,h}(z)\Phi_{e,h}(xc). \tag{33}$$

The complete potential which describes piezoelectric effects and local exchange-correlation potential in quantum well one can find as follows

$$\Phi(z) = \Phi^H_h(z) + \Phi^H_e(z) + \Phi^H_h(z)\Phi_h(xc) + \Phi^H_e(z)\Phi_e(xc). \tag{34}$$

4 Uncertainty Heisenberg principle

The Heisenberg equation for a microscopic dipole $\hat{p}^{\nu_e\nu_h}_{\mathbf{p}} = \langle\hat{b}_{-\mathbf{p}}\hat{a}_{\mathbf{p}}\rangle$ due to an electron-hole pair with the electron (hole) momentum **p** (–**p**) and the subband number ν_e (ν_h) is written in the form:

$$\frac{\partial\hat{p}^{\nu_e\nu_h}_{\mathbf{p}}}{\partial t} = \frac{i}{\hbar}[\hat{H},\hat{p}^{\nu_e\nu_h}_{\mathbf{p}}]. \tag{35}$$

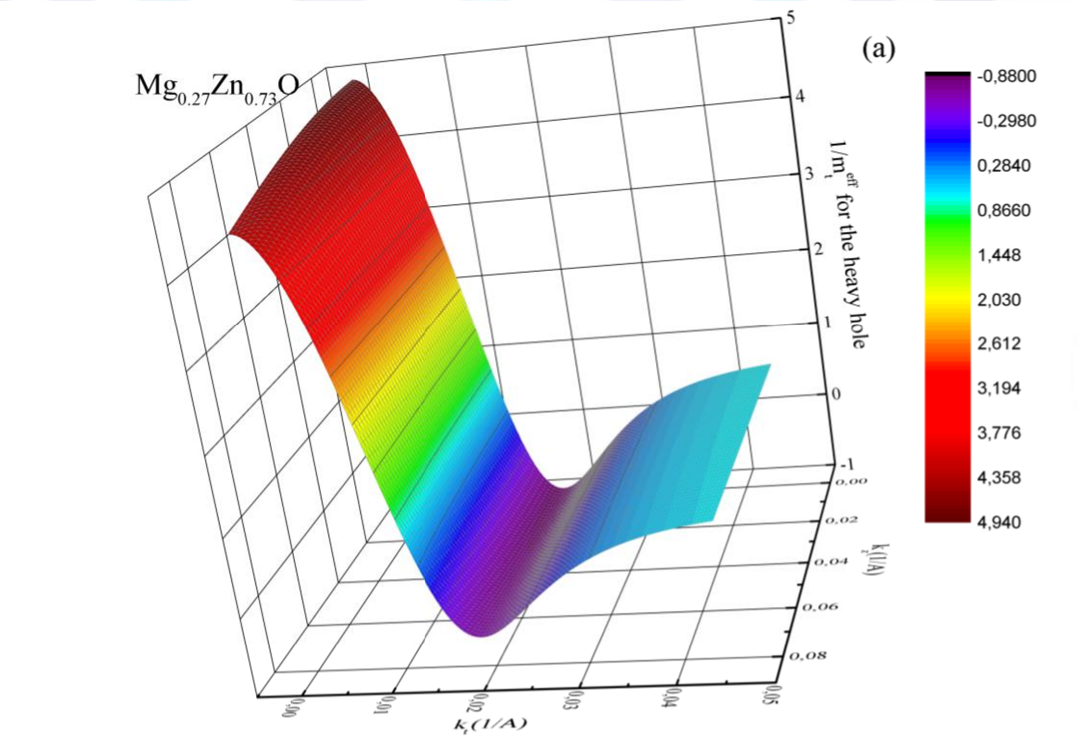

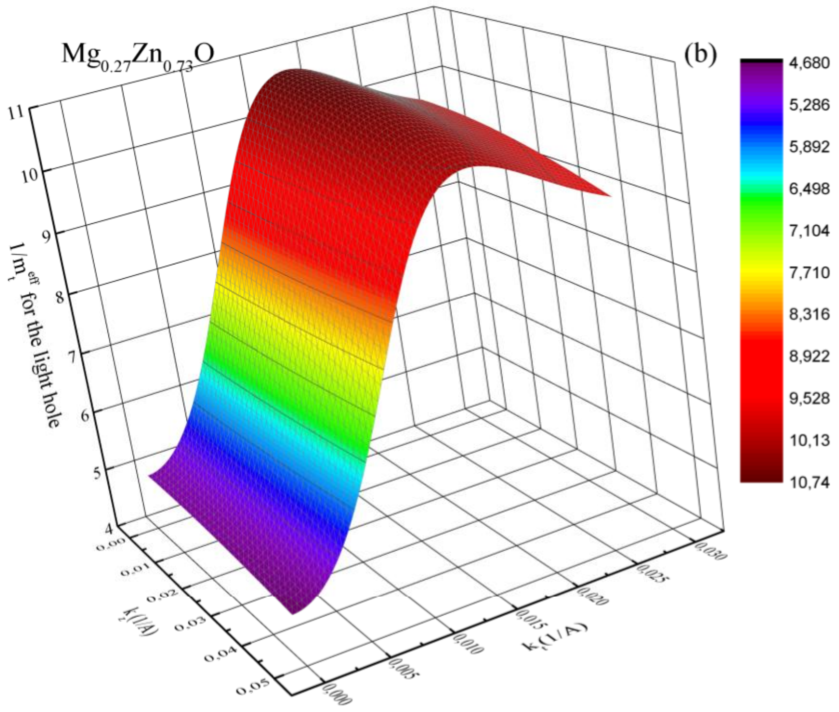

Figure 3: (Color online) The transverse effective masses for $Mg_{0.27}Zn_{0.73}O$ under biaxial strain: (a) for the heavy hole; (b) for the light hole.

We assume a nondegenerate situation described by the Hamiltonian $\hat{H} = \hat{H}_0 + \hat{V} + \hat{H}_{int}$, which is composed of the kinetic energy of an electron $\varepsilon_{e,\mathbf{p}}^{\nu_e}$ and the kinetic energy of a hole $\varepsilon_{h,\mathbf{p}}^{\nu_h}$ in the electron-hole representation:

$$\hat{H}_0 = \sum_{\mathbf{p}} \varepsilon_{e,\mathbf{p}}^{\nu_e} \hat{a}_{\mathbf{p}}^{+} \hat{a}_{\mathbf{p}} + \varepsilon_{h,\mathbf{p}}^{\nu_h} \hat{b}_{-\mathbf{p}}^{+} \hat{b}_{-\mathbf{p}}, \tag{36}$$

where **p** is the transversal quasimomentum of carriers in the plane of the quantum well, $\hat{a}_{\mathbf{p}}$, $\hat{a}_{\mathbf{p}}^{+}$, $\hat{b}_{-\mathbf{p}}$, and $\hat{b}_{-\mathbf{p}}^{+}$ are the annihilation and creation operators of an electron and a hole. The Coulomb interaction Hamiltonian for particles in the electron-hole representation takes the form:

$$\hat{V} = \frac{1}{2} \sum_{\mathbf{p},\mathbf{k},\mathbf{q}} V_q^{\nu_e \nu_e \nu_e \nu_e} \hat{a}_{\mathbf{p}+\mathbf{q}}^{+} \hat{a}_{\mathbf{k}-\mathbf{q}}^{+} \hat{a}_{\mathbf{k}} \hat{a}_{\mathbf{p}} +$$

$$+ V_q^{\nu_h \nu_h \nu_h \nu_h} \hat{b}_{\mathbf{p}+\mathbf{q}}^{+} \hat{b}_{\mathbf{k}-\mathbf{q}}^{+} \hat{b}_{\mathbf{k}} \hat{b}_{\mathbf{p}} -$$

$$- 2V_q^{\nu_e \nu_h \nu_h \nu_e} \hat{a}_{\mathbf{p}+\mathbf{q}}^{+} \hat{b}_{\mathbf{k}-\mathbf{q}}^{+} \hat{b}_{\mathbf{k}} \hat{a}_{\mathbf{p}}, \tag{37}$$

where

$$V_q^{\nu_\alpha \nu_\beta \nu_\beta \nu_\alpha} = \frac{e^2}{\kappa} \frac{1}{A} \int_{-w/2}^{+w/2} dz \int_{-w/2}^{+w/2} dz' \chi_{\nu_\alpha}(z) \chi_{\nu_\beta}(z') \frac{2\pi}{q} \times$$

$$\times e^{-q|z-z'|} \chi_{\nu_\beta}(z') \chi_{\nu_\alpha}(z), \tag{38}$$

is the Coulomb potential of the quantum well, κ is the dielectric permittivity of a host material of the quantum well, and A is the area of the quantum well in the xy plane.

The Hamiltonian of the interaction of a dipole with an electromagnetic field is described as follows:

$$\hat{H}_{int} = -\frac{1}{A}\sum_{\nu_e,\nu_h,\mathbf{p}}((\mu_{\mathbf{p}}^{\nu_e\nu_h})^* \hat{p}_{\mathbf{p}}^{\nu_e\nu_h} E^* e^{i\omega t} + + (\mu_{\mathbf{p}}^{\nu_e\nu_h})(\hat{p}_{\mathbf{p}}^{\nu_e\nu_h})^+ E e^{-i\omega t}), \quad (39)$$

where $\hat{p}_{\mathbf{p}}^{\nu_e\nu_h} = \langle \hat{b}_{-\mathbf{p}} \hat{a}_{\mathbf{p}} \rangle$ is a microscopic dipole due to an electron-hole pair with the electron (hole) momentum **p** (–**p**) and the subband number ν_e (ν_h), $\mu_{\mathbf{k}}^{\nu_e\nu_h} = \int d^3 r U_{j'\sigma'\mathbf{k}} \mathbf{e}\hat{\mathbf{p}} U_{j\sigma\mathbf{k}}$, is the matrix element of the electric dipole moment, which depends on the wave vector **k** and the numbers of subbands, between which the direct interband transitions occur, $\mathbf{e}$ is a unit vector of the vector potential of an electromagnetic wave, $\hat{\mathbf{p}}$ is the momentum operator. Subbands are described by the wave functions $U_{j'\sigma'\mathbf{k}}$, $U_{j\sigma\mathbf{k}}$, where j' is the number of a subband from the conduction band, σ' is the electron spin, j is the number of a subband from the valence band, and σ is the hole spin. We consider one lowest conduction subband $j'=1$ and one highest valence subband $j=1$. E and ω are the electric field amplitude and frequency of an optical wave.

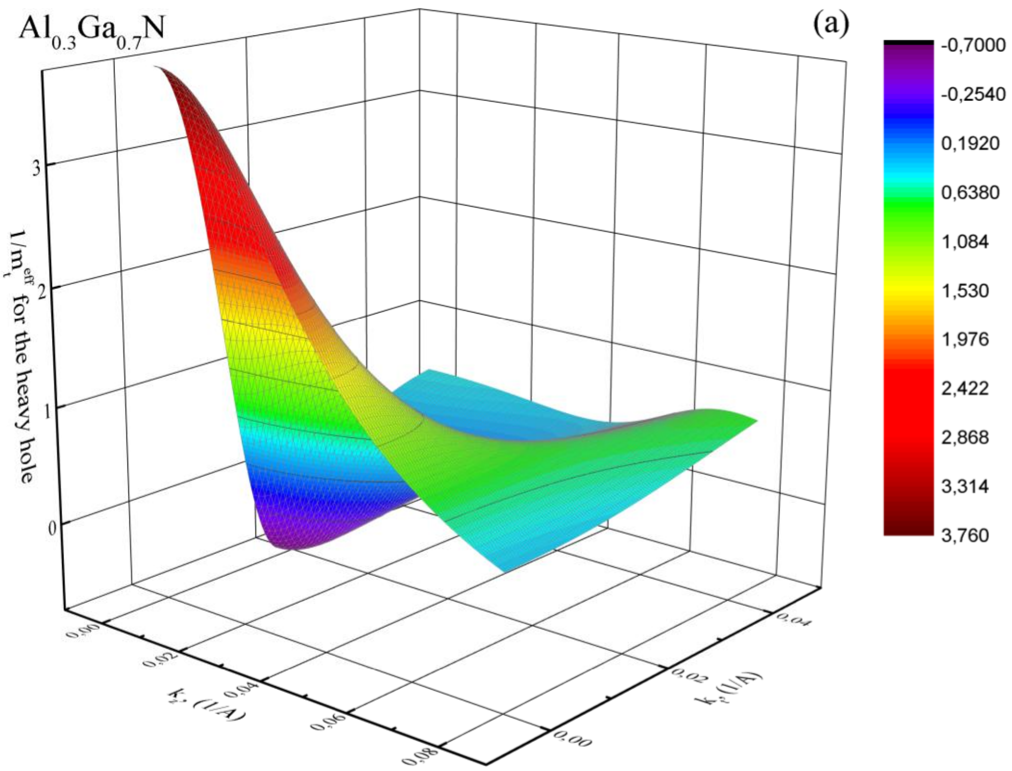

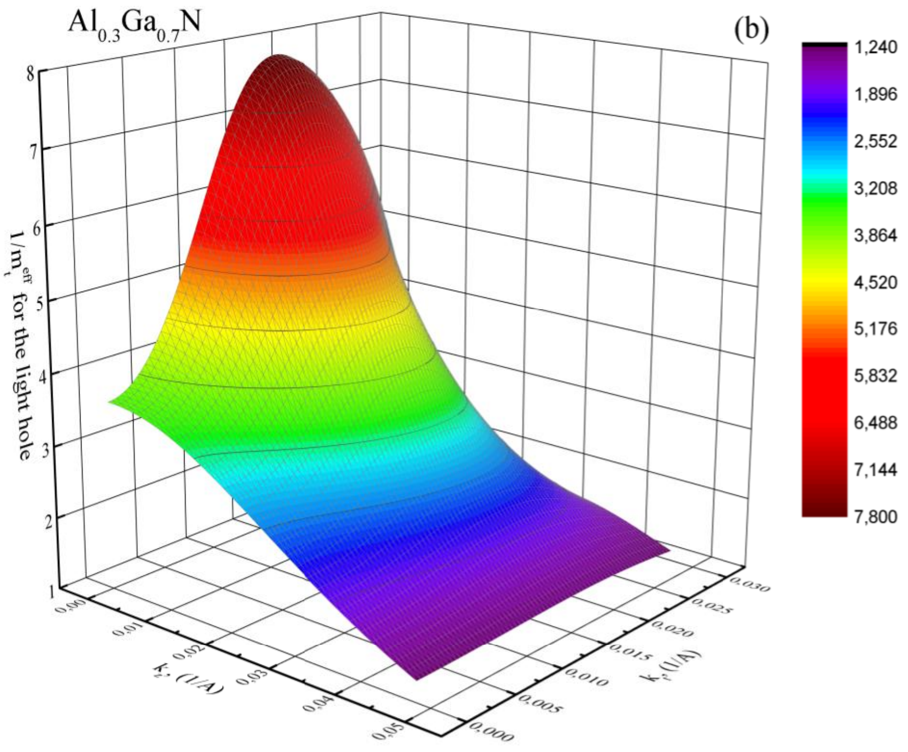

Figure 4: (Color online) The transverse effective masses for $Al_{0.3}Ga_{0.7}N$ under biaxial strain: (a) for the heavy hole; (b) for the light hole.

The polarization equation for the wurtzite quantum well in the Hartree–Fock approximation with regard for the wave functions for an electron and a hole written in the form [12,23], where the coefficients of the expansion of the wave function of a hole in the basis of wave functions (known as spherical functions) with the orbital angular momentum $l = 1$ and the eigenvalue m_l of its z component, depend on the wave vector can look for as follows:

$$\frac{d\hat{p}_{\mathbf{p}}^{\nu_e\nu_h}}{dt} = -i\omega_{\mathbf{p}}^{\nu_e\nu_h}\hat{p}_{\mathbf{p}}^{\nu_e\nu_h} - i\Omega_{\mathbf{p}}^{\nu_e\nu_h}(-1+\hat{n}_{\mathbf{p}}^{\nu_e}+\hat{n}_{\mathbf{p}}^{\nu_h}). \tag{40}$$

The transition frequency $\omega_{\mathbf{p}}^{\nu_e\nu_h}$ and the Rabi frequency with regard for the wave function [12,23] are described as

$$\omega_{\mathbf{p}}^{\nu_e\nu_h} = \frac{1}{\hbar}(\varepsilon_{g0} + \varepsilon_{e,\mathbf{p}}^{\nu_e} + \varepsilon_{h,\mathbf{p}}^{\nu_h}), \tag{41}$$

$$\Omega_{\mathbf{p}}^{\nu_e\nu_h} = \frac{1}{\hbar}(\mu_{\mathbf{p}}^{\nu_e\nu_h}Ee^{-i\omega t} + \sum_q V_{\left\{\begin{array}{c}|-\mathbf{p}|\\|-\mathbf{p}-\mathbf{q}|\end{array}\right\}}^{\nu_e\nu_h\nu_h\nu_e})\hat{p}_{\mathbf{p}+\mathbf{q}}^{\nu_e\nu_h}, \tag{42}$$

where $\varepsilon_{e,\mathbf{p}}^{\nu_e}, \varepsilon_{h,\mathbf{p}}^{\nu_h}$ - Hartree-Fock energies for electron and holes,

$$V_{\left\{\begin{array}{c}|-\mathbf{p}|\\|-\mathbf{p}-\mathbf{q}|\end{array}\right\}}^{\nu_e\nu_h\nu_h\nu_e} = \frac{1}{2}\frac{e^2}{\kappa}\frac{1}{2\pi}\int_0^{2\pi}d\varphi\sum_\alpha g_\alpha\int dq\times$$

$$\times \int dz_{\xi} \int dz_{\xi'} \chi_{n_1}(z_{\xi}) \chi_{m_1}(z_{\xi'}) \chi_{m_2}(z_{\xi'}) \chi_{n_2}(z_{\xi}) \times$$

$$\times e^{-q|z_{\xi}-z_{\xi'}|} C_p^j[n_1,1] V_p^j[m_1,1] C_{Q_1}^i[n_2,1] V_{Q_1}^i[m_2,1],$$

$$n_1 = m_1 = n_2 = m_2 = 1,$$

$$\mathbf{Q}_1 = \mathbf{q} + \mathbf{p}, \tag{43}$$

where $\chi_{n_1}(z_{\xi})$ is the envelope of the wave functions of the quantum well, $V_p^i[m_1,1]$ and $C_p^j[n_1,1]$ are coefficients of the expansion of the wave functions of a hole and electron at the envelope part, φ is the angle between the vectors $\mathbf{p}$ and $\mathbf{q}$, and g_{α} is a degeneracy order of a level.

Numerically solving this integro-differential equation, we can obtain the absorption coefficient of a plane wave in the medium from the Maxwell equations:

$$\alpha(\omega) = \frac{\omega}{\kappa n c E} \mathrm{Im} P, \tag{44}$$

where c the velocity of light in vacuum, n is a background refractive index of the quantum well material,

$$P = \frac{2}{A} \sum_{\nu_e, \nu_h, \mathbf{p}} (\mu_{\mathbf{p}}^{\nu_e \nu_h})^* p_{\mathbf{p}}^{\nu_e \nu_h} e^{i\omega t}. \tag{45}$$

The light absorption spectrum presented in the paper in Fig. 7, reflects only the strict TE (*x* or *y*) light polarization.

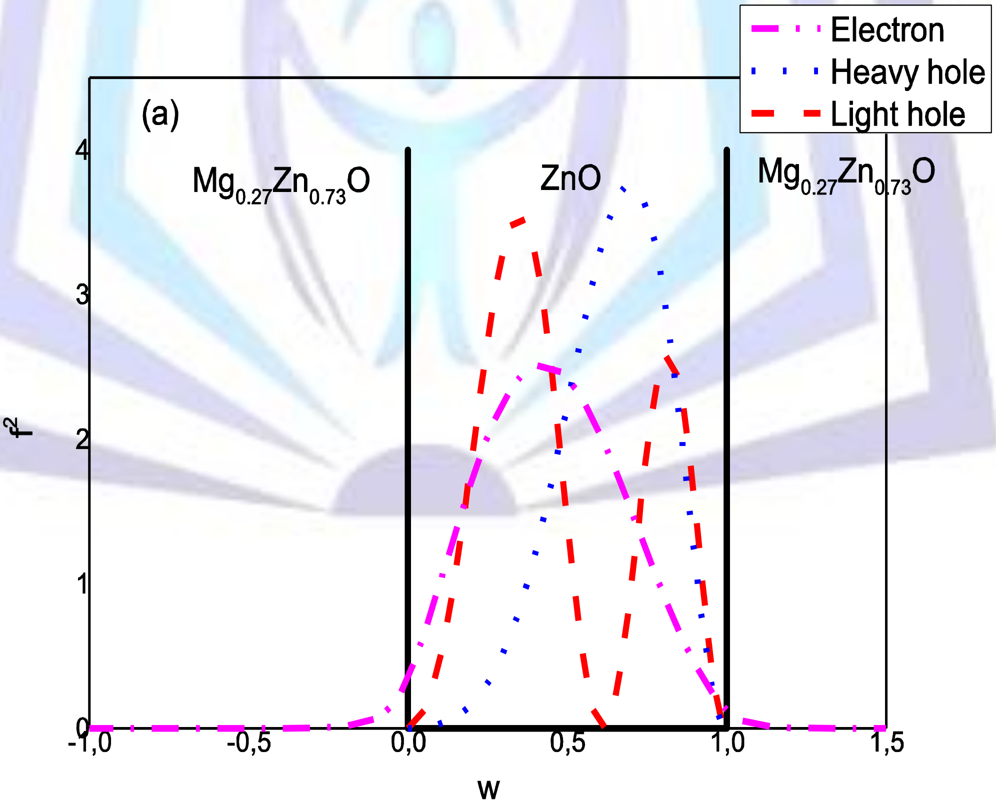

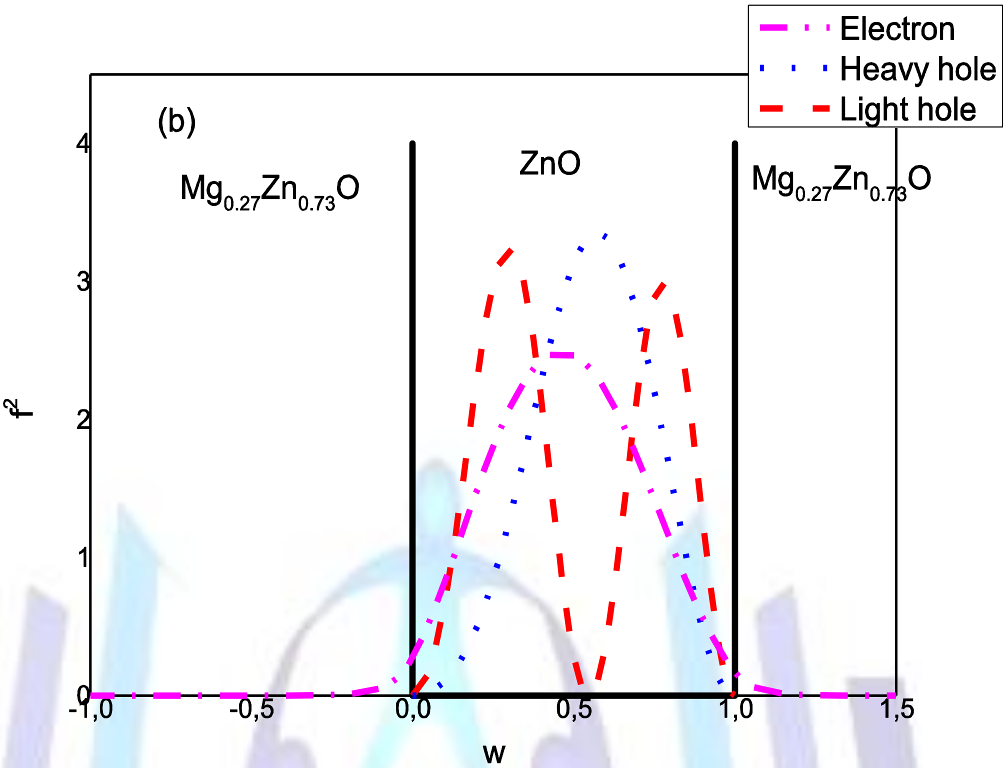

Figure 5: (Color online) For the quantum well $ZnO/Mg_{0.27}Zn_{0.73}O$ with a width 4 nm, at a carriers concentration $4*10^{12}$ cm $^{-2}$, at a temperature 300 K, at a transverse wave vector $k_t = 2*10^7$ cm $^{-1}$: (a) Square of Hartree wave functions; (b) Square of Hartree-Fock wave functions.

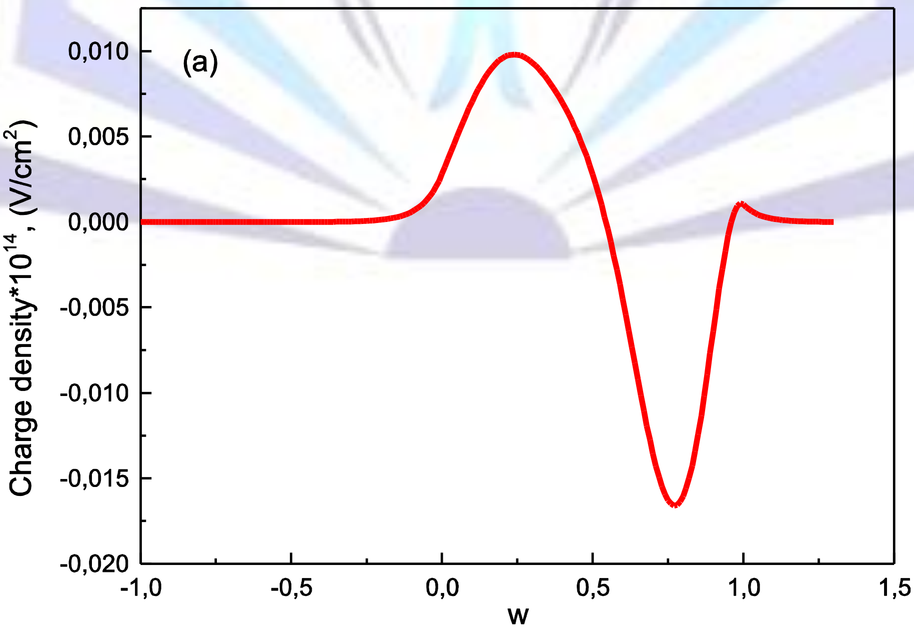

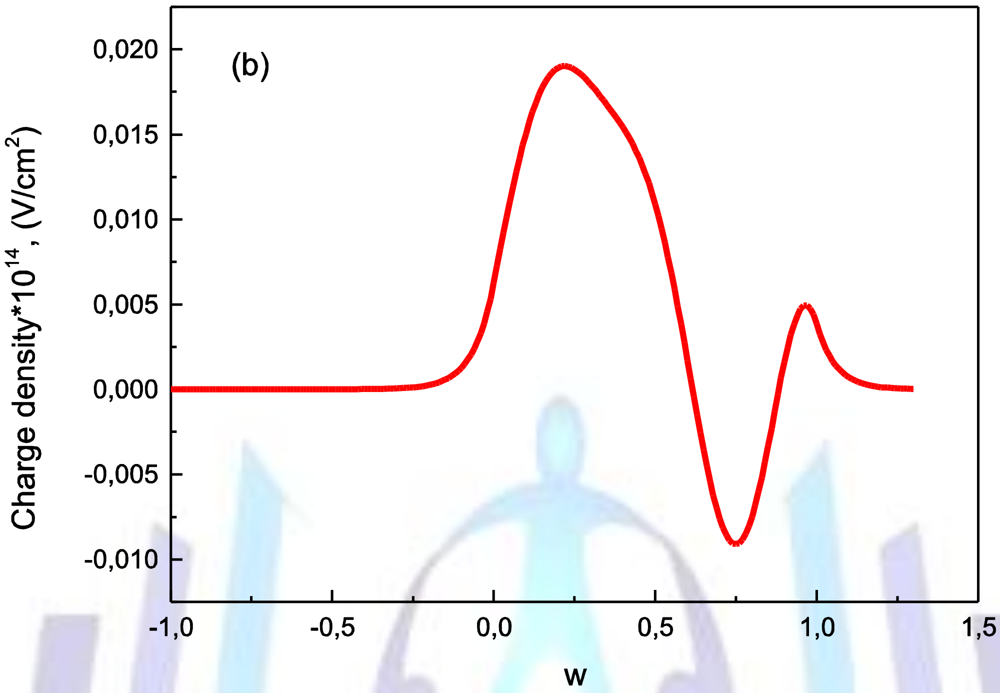

Figure 6: (Color online) For the quantum well $ZnO/Mg_{0.27}Zn_{0.73}O$ with a width 4 nm, at a carriers concentration $4*10^{12}$ cm $^{-2}$, at a temperature 300 K: (a) Hartree charge density; (b) Hartree-Fock charge density.

From Uncertainty Heisenberg principle:

$$\Delta x \Delta p \geq \frac{\hbar}{2}, \qquad (46)$$

can be found the localization range particle-hole pair $\Delta x \geq \frac{\hbar}{4mc}$.

Table 1. The localization range particle-hole pair Δx in cm, exciton binding energy Ry in meV, carriers concentration $n = p$ in cm $^{-2}$, Bohr radius a_B in cm.

Δx	Ry	n=p	a_B
$5.58*10^{-11}$	38.53	$4*10^{12}$	$2.39*10^{-7}$

Hence the Bohr radius is grater than the localization range particle-hole pair, and the excitons may be spontaneously created.

5 Results and discussions

We consider QCSE in strained würtzite $ZnO/Mg_{0.27}Zn_{0.73}O$ quantum well with width 4 nm, in which the barrier height is a constant value for electrons and is equal to $U_0 = 536.22$ meV. The theoretical analysis of piezoelectric effects and exchange-correlation effects is based on the self-consistent solution of the Schrödinger equations for electrons and holes in quantum well of width w with including Stark effect and the Poisson equations. The one-dimensional Poisson equation contains the Hartree potential which includes the one-dimensional charge density for electrons and holes along the polarization field distribution. The three-dimensional Poisson equation contains besides the one-dimensional charge density for electrons and holes along the polarization field distribution the exchange-correlation potential which is built on convolutions of a plane-wave part of wave functions in addition. All calculations are performed at a temperature of 300 K.

We have calculated carriers population of the lowest conduction band and the both heavy hole and light hole valence band. Solving (13) for holes in the infinitely deep quantum well and finding the minimum of functional (17) for electrons in a quantum well with barriers of finite height, we can find the energy and wave functions of electrons and holes with respect to Hartree potential and exchange-correlational potential in a piezoelectric field at a carriers concentration $n = p = 4*10^{12}$ cm $^{-2}$. The screening field is determined by iterating Eqs. (13), (17), (22) until the solution of energy spectrum is converged.

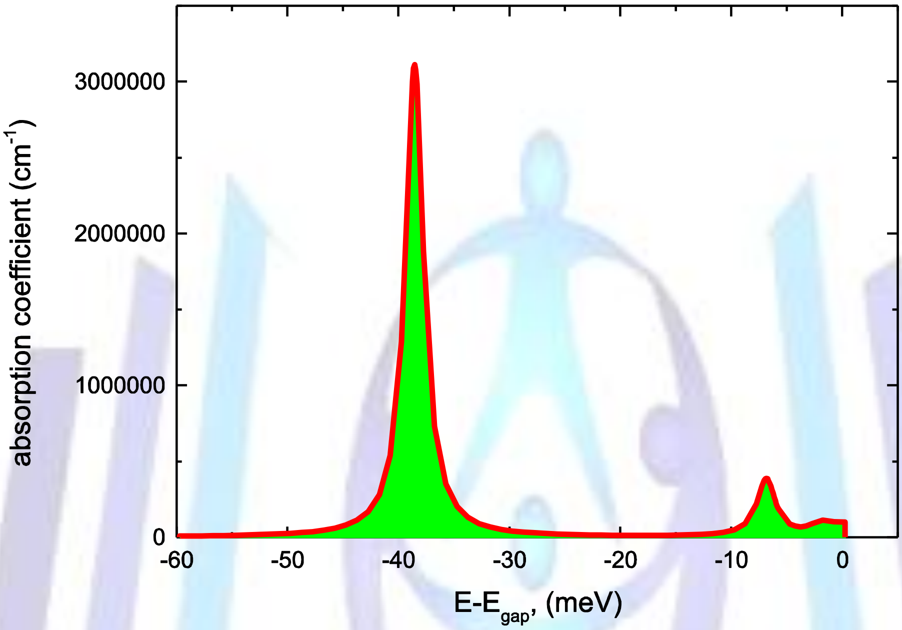

Figure 7: (Color online) Absorption coefficient for the quantum well $ZnO/Mg_{0.27}Zn_{0.73}O$ with a width 4 nm, at a carriers concentration $4*10^{12}$ cm $^{-2}$, at a temperature 300 K.

The dispersion of the renormalization band gap is presented in Fig. 1. We have found $E_g^H - E_g^{Flatband} = 20.72$ meV, $E_g^{HF} - E_g^H = 4.40$ meV, comparing the Hartree band gap with the flat band gap as well as the Hartree band gap with the Hartree-Fock band gap. Comparing E_g^{HF} and E_g^H and a shape of bedplate of quantum well for electrons which is presented in Fig. 2 as well as a same shape of bedplate of quantum well for holes one can see that an electron mass is less than a hole mass. The effective masses $Mg_{0.27}Zn_{0.73}O$ under biaxial strain for the heavy holes and light holes are presented in Fig. 3. Both the effective mass of $Mg_{0.27}Zn_{0.73}O$ under biaxial strain for the heavy hole and the effective mass of $Al_{0.3}Ga_{0.7}N$ under biaxial strain for the heavy hole are presented in Fig. 4. From these Figures one can see that a mass of heavy hole of $Mg_{0.27}Zn_{0.73}O$ is greater than a mass of heavy hole of $Al_{0.3}Ga_{0.7}N$. Comparing the effective mass of $Mg_{0.27}Zn_{0.73}O$ under biaxial strain for the heavy hole with an effective-mass parameter $A_1 = -2.743$ one can conclude that an effective mass of heavy hole of $Mg_{0.27}Zn_{0.73}O$ under biaxial strain is greater than an effective-mass of heavy hole of ZnO.

The squares of Hartree and Hartree-Fock wave functions for electrons, heavy holes and light holes are presented in Fig. 5. From Fig. 5 one can conclude that an overlap integrals of the wave functions of holes and electron taking into the account besides the piezoelectric effects the exchange-correlation effects in addition are greater than an overlap integrals of Hartree ones. Hartree charge density distribution and Hartree-Fock charge density distribution are presented in Fig. 6. Comparing charge density distributions presented in Fig. 6 one can conclude that Hartree particles distribute greater on edges of quantum well than Hartree-Fock particles.

It is found that the localization range particle-hole pair $\Delta x \geq \frac{\hbar}{4mc}$:$5.58*10^{-11}$ cm. Exciton binding energy is equal Ry=38.53 meV at carriers concentration $n = p = 4*10^{12}$ cm $^{-2}$. Bohr radius is equal $a_B = 2.39*10^{-7}$ cm.

If the Bohr radius is grater than the localization range particle-hole pair, the excitons may be spontaneously created.

6 Creation of beelectron of Dirac cone: the tachyon solution in magnetic field.

The graphene [24-26] presents a new state of matter of layered materials. The energy bands for graphite was found using "tight-binding" approximation by P.R. Wallace [27]. In the low-energy limit the single-particle spectrum is Dirac cone similarly to the light cone in relativistic physics, where the light velocity is substituted by the Fermi velocity v_F and describes by the massless Dirac equation.

The graphene is the single graphite layer, i. e. two-dimensional graphite plane of thickness of single atom. The graphene lattice resembles a honeycomb lattice. The graphene lattice one can consider like into the composite of two triangular sublattices. In 1947 Wallace in "tight-binding" approximation consider a graphite which consist off the graphene blocks with taken into account the overlap only the nearest π -electrons.

The two-dimensional nature of graphene and the space and point symmetries of graphene acquire of the reason for the massless electron motion since lead into massless Dirac equation (Majorana fermions) [27,28]. At low-energy limit the single particle spectrum forms with π -electron carbon orbital and consist off completely occupation valence cone and completely empty conduction cone, which have cone like shape with single Dirac point. In Dirac point the existing an electron as well as a hole is proved. The state in Dirac cone is double degenerate with taken into account a spin.

The existing of the massless Dirac fermions in graphene was proved based on the unconventional quantum Hall effect. The reason of creation the integer Hall conductivity [29-32] is derived from Berry phase [33,34].

When the magnetic field is applied perpendicularly into graphene plane the lowest (n=0) Landau level has the energy $\pm\Delta$ in two nonequivalent cones $K_{\mp}$, correspondingly [35]. In the paper [35] the Dirac mass via a splitting value is found when Zeeman coupling is absence. These properties of the lowest Landau level which distribute between particles and antiparticles in equal parts are base of the integer quantum Hall effect in graphene [35]. For $n \geq 1$ an all Landau levels are fourfold degenerate. For $n = 0$ a states in both cones are twofold degenerate with energies $\pm\Delta$ with taken into account a spin [35].

7 Solution of massless chiral Dirac equation for pair of two Majorana fermions coupled via a Coulomb potential in magnetic field in Landau gauge.

Calculate the quantized Landau energy as well as the wave function of the Majorana particles in cylindrical coordinate in magnetic field in Landau gauge. Enter the production and annihilation operators as following:

$$\begin{aligned} \hat{c}^{\dagger} &= \sqrt{B}(-\frac{\partial}{\partial \xi_2} + \xi_1), \\ \hat{c} &= \sqrt{B}(\frac{\partial}{\partial \xi_1} + \xi_2), \end{aligned} \tag{47}$$

where $\xi_1 = \frac{\sqrt{B}}{2}\zeta$, $\xi_2 = \frac{\sqrt{B}}{2}\eta$, $\zeta = x + iy$, $\eta = x - iy$, which satisfies the commutator relation:

$$[\hat{c}^{\dagger}, \hat{c}] = 2B. \tag{48}$$

Hence the Coulomb potential may be found in the form [36]:

$$V(\rho) = \hbar v_F \frac{\alpha}{\rho}. \tag{49}$$

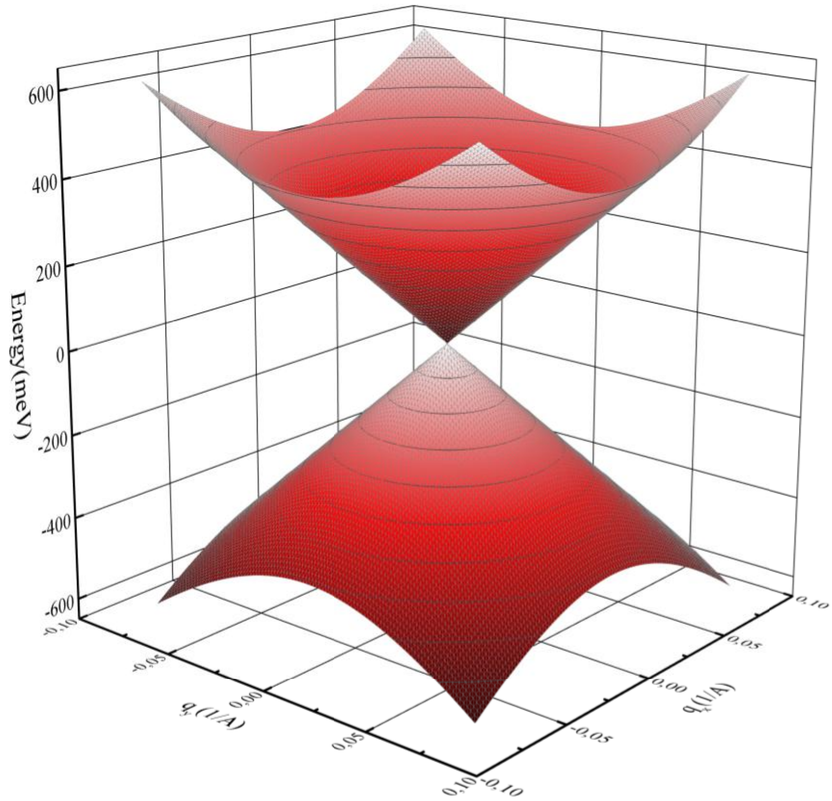

Figure 8: (Color online) Single-particle spectrum of graphene for massless Dirac fermions (Majorana fermions).

When magnetic field is applied perpendicularly into graphene plane in z axis along field distribution. The vector potential in the gauge [20] $\mathbf{A} = \frac{1}{2}[\mathbf{Hr}]$ has a components $A_\varphi = H\rho/2$, $A_\rho = A_z = 0$ and Schrödinger equation:

$$-4\frac{\partial^2\Psi}{\partial\rho^2} - \frac{4}{\rho}\frac{\partial\Psi}{\partial\rho} - \frac{4}{\rho^2}\frac{\partial^2\Psi}{\partial\varphi^2} - \frac{4i}{\rho^2}\frac{\partial\Psi}{\partial\varphi}$$
$$-2iB\frac{\partial\Psi}{\partial\varphi} + \frac{B^2}{4}\rho^2\Psi - 2B\Psi = 2\varepsilon^2\Psi. \tag{50}$$

The solution Eq. (50) can look for in the form:

$$\Psi_{n,k} = \frac{1}{\sqrt{2\pi}}R(\rho)e^{im\varphi}. \tag{51}$$

Substituting the solution in Eq. (50), one can find for the radial function the following equation

$$R'' + \frac{1}{\rho}R' + (\beta - \frac{k^2}{\rho^2} - 2\gamma m - \gamma^2\rho^2)R = 0, \tag{52}$$

where $\beta = (\varepsilon^2 + B)/2$, $\gamma = B/4$, $k^2 = m^2 + m - \alpha^2$. Entering the new independent variable $\xi = \gamma\rho^2$, the equation (50) can be rewritten in the form:

$$\xi R'' + R' + (\frac{\xi}{4} + \lambda - \frac{k^2}{4\xi})R = 0, \tag{53}$$

where $\lambda = \frac{\beta}{4\gamma} - \frac{m}{2}$. At $\xi \to \infty$ conduct of sought for function are shown to be found as following $e^{-\xi/2}$, and at $\xi \to 0$ like $\xi^{k/2}$.

The solution of the Eq. (53) can look for in the form:

$$R = e^{-\xi/2}\xi^{k/2}\varpi(\xi), \tag{54}$$

for $\varpi(\xi)$ we derive the equation for confluent hypergeometric function:

$$\varpi = F(-(\lambda - \frac{k+1}{2}), k+1, \xi). \tag{55}$$

From the condition of finite of the wave function one can find the energy spectrum in the form:

$$\varepsilon = \pm B\sqrt{l}, \tag{56}$$

where $l = 2n + m + k$, $n, m = 0,1,2,3,...$. The wave function expressed via the associated Laguerre polynomial:

$$R_{n,k} = [\frac{B(n-k)!}{2n!^3(n-k+1)}]^{1/2}\psi_{n,k}, \tag{57}$$

where

$$\psi_{n,k} = e^{-\frac{\xi}{2}}\xi^{\frac{k}{2}}L_n^k(\xi), \tag{58}$$

Entering the production and annihilation operators as following (47) and solving Schrödinger equation one can derive the known for quantum electrodynamics (QED) solution - the root ambiguity in energy spectrum $\varepsilon = \pm B\sqrt{l}$, where l is a number of natural numbers set [37]. The root ambiguity in energy spectrum at the solution of the problem about quantization with relativistic invariance lead in quantum field theory into the creation of a pairs of particles (particles+antiparticles) [38]. When l is a number of complex numbers set the tachyon solutions are provided by arising the complex energy in spectrum of quantization of Landau for pair of two Majorana fermions coupled via a Coulomb potential.

For graphene with strong Coulomb interaction the Bethe-Salpeter equation for the electron-hole bound state was solved and a tachyonic solution was found [39].

8 Appendix

C_{6v}	E	C_2	$2C_3$	$2C_6$	$3\sigma_v$	$3\sigma_v'$	
Γ_1	1	1	1	1	1	1	k_z^2, k_t^2, J_z^2, I
Γ_2	1	1	1	-1	-1	-1	J_z, σ_z
Γ_3	1	1	-1	1	1	-1	
Γ_4	1	1	-1	-1	-1	1	
Γ_5	2	-1	0	-2	1	0	$k_+, k_-, \sigma_+, \sigma_-$
Γ_6	2	-1	0	2	-1	0	$k_+^2, k_-^2, J_+^2, J_-^2$

where $k_{\pm} = k_x \pm ik_y$, $k_t^2 = k_x^2 + k_y^2$, $J_{\pm} = \frac{1}{\sqrt{2}}(J_x \pm iJ_y)$, $2[J_z J_{\pm}] = J_z J_{\pm} + J_{\pm} J_z$, $\sigma_{\pm} = \frac{1}{2}(\sigma_x \pm \sigma_y)$.

9 Conclusions

In this paper a theoretical studies of the space separation of electron and hole wave functions in the quantum well $ZnO/Mg_{0.27}Zn_{0.73}O$ by the self-consistent solution of the Schrödinger equations for electrons and holes and the Poisson equations at the presence of spatially varying quantum well potential due to the piezoelectric effect and local exchange-correlation potential are presented. The exchange-correlation potential energy is found from the solution of three-dimensional Poisson's equation, using both an expression by Gunnarsson and Lundquist [22], and following criterions. The criterion $k_F > \sqrt{n}/4$ at carrier densities $4*10^{12}$ cm $^{-2}$, at a temperature T=0 K is carried as $1 > 0.1$. The criterion does not depend from a width of well. The solution of equations system (13), (17), (23) as well as (13), (17), (22) does not depend from a temperature. The ratio of Coulomb potential energy to the Fermi energy is $r_s = E_C/E_F = 0.63 < 1$. The one-dimensional Poisson equation contains the Hartree potential which includes the one-dimensional charge density for electrons and holes along the polarization field distribution. The three-dimensional Poisson equation contains besides the one-dimensional charge density for electrons and holes along the polarization field distribution the exchange-correlation potential which is built on convolutions of a plane-wave part of wave functions in addition. The problem consists of the one-dimensional Poisson's equation solving of which may be found Hartree potential energy and three-dimensional Poisson's equation which is separated on one-dimensional and two-dimensional equations by separated of variables. At the condition that the ratio of wave function localization in the longitudinal z direction on transversal in-plane wave function localization is less 1. We have compared the Hartree band gap with the flat band gap as well as the Hartree band gap with the Hartree-Fock band gap and have found $E_g^H - E_g^{Flatband} = 20.72$ meV, $E_g^{HF} - E_g^H = 4.40$ meV. An overlap integrals of the wave functions of holes and electron taking into account besides the piezoelectric effects the exchange-correlation effects in addition is greater than an overlap integral of Hartree ones. The Hartree particles distribute greater on edges of quantum well than Hartree-Fock particles. It is found that an effective mass of heavy hole of $Mg_{0.27}Zn_{0.73}O$ under biaxial strain is greater than an effective-mass of heavy hole of ZnO. It is calculated that an electron mass is less than a hole mass. It is found that the Bohr radius is grater than the localization range particle-hole pair, and the excitons may be spontaneously created.

Schrödinger equation for pair of two massless Dirac particles when magnetic field is applied in Landau gauge is solved exactly. Landau quantization $\varepsilon = \pm B\sqrt{l}$ for pair of two Majorana fermions coupled via a Coulomb potential from massless chiral Dirac equation in cylindric coordinate is found. In this case the separation of center of mass and relative motion is derived. The root ambiguity in energy spectrum leads into Landau quantization for beelectron, when the states in which the one simultaneously exists are allowed. The tachyon solution with imaginary energy in Cooper problem ($\varepsilon^2 < 0$) is found. The wave function are shown to be expressed via the associated Laguerre polynomial. In the paper the Cooper problem in superconductor theory is solved as quantum-mechanical problem for two electrons unlike from the paper [39] where the Bethe-Salpeter equation was solved for electron-hole pair.

REFERENCES

[1] A. Bakin, A. El-Shaer, A. C. Mofor, M. Al-Suleiman, E. Schlenker and A. Waag, Phys. Status Solidi C **4**, 158 (2007).

[2] J. Zippel, M. Stölzer, A. Müller, G. Benndorf, M. Lorenz, H. Hochmuth, and M. Grundmann, Phys. Status Solidi B **247**, 398 (2010).

[3] T. V. Shubina, A. A. Toropov, O. G. Lublinskaya, P. S. Kopev, S. V. Ivanov, A. El-Shaer, M. Al-Suleiman, A. Bakin, A. Waag, A. Voinilovich, E. V. Lutsenko, G. P. Yablonskii, J. P. Bergman, G. Pozina, and B. Monemar, Appl. Phys. Lett. **91**, 201104 (2007).

[4] S. -M. Li, B. -J. Kwon, H. -S. Kwack, L. -H. Jin, Y. -H. Cho, Y. -S. Park, M. -S. Han, and Y. -S. Park, J. Appl. Phys. **107**, 033513 (2010).

[5] G. Tabares, A. Hierro, B. Vinter, and J. -M. Chauveau, Appl. Phys. Lett. **99**, 071108 (2011).

[6] J. W. Sun and B. P. Zhang, Nanotechnology **19**, 485401 (2008).

[7] J. -M. Chauveau, M. Laügt, P. Vennegues, M. Teisseire, B. Lo, C. Deparis, C. Morhain, B. Vinter, Semicond. Sci. Technol. **23**, 035005 (2008).

[8] T. A. Wassner, B. Laumer, S. Maier, A. Laufer, B. K. Meyer, M. Stutzmann, M. Eickhoff, J. Appl. Phys. **105**, 023505 (2009).

[9] A. Chernikov, S. Schäfer, M. Koch, S. Chatterjee, B. Laumer, M. Eickhoff, Phys. Rev. B **87**, 035309 (2013).

[10] Almamun Ashrafi, J. Appl. Phys. **107**, 123527 (2010).

[11] J. Wang, J. B. Jeon, Yu. M. Sirenko, K. W. Kim, Photon. Techn. Lett. **9**, 728 (1997).

[12] L. O. Lokot, Ukr. J. Phys. **57**, 12 (2012), arXiv:1302.2780v1 [cond-mat.mes-hall], 2013.

[13] G. L. Bir, G. E. Pikus *Symmetry and Strain-Induced Effects in Semiconductors* (Wiley, New York, 1974).

[14] D. W. Langer, R. N. Euwema, Koh Era, Takao Koda, Phys. Rev. B **2**, 4005 (1970).

[15] P.Y. Yu and M. Cardona, *Fundamentals of Semiconductors* (Springer, Berlin, 1996).

[16] Qimin Yan, Patrick Rinke, M. Winkelnkemper, A. Qteish, D. Bimberg, Matthias Scheffer, Chris G. Van de Walle, Semicond. Sci. Technol. **26**, 014037 (2011).

[17] *Semiconductors*, edited by O. Madelung (Springer, Berlin, 1991).

[18] S. L. Chuang and C. S. Chang, Phys. Rev. B **54**, 2491 (1996).

[19] G. Bastard, E. E. Mendez, L. L. Chang, L. Esaki, Phys. Rev. B **28**, 3241 (1983).

[20] L. D. Landau, E. M. Lifshitz Quantum Mechanics. Non-Relativistic Theory (Pergamon, NewYork, 1977).

[21] T. Makino, Y. Segawa, M. Kawasaki, H. Koinuma, Semicond. Sci. Tech. **20**, S78 (2005), arXiv: cond-mat/0410120v2 [cond-mat.mtrl-sci].

[22] O. Gunnarsson, B. I. Lundqvist, Phys. Rev. B **13**, 4274 (1976).

[23] L.O. Lokot, Ukr. J. Phys. **54**, 963 (2009).

[24] K. S. Novoselov, A. K. Geim, S. V. Morozov, D. Jiang, M. I. Katsnelson, I. V. Grigorieva, S. V. Dubonos, A. A. Firsov, Nature **438**, 197 (2005).

[25] F. T. Vasko, V. Ryzhii, Phys. Rev. B **77**, 195433 (2008).

[26] Y. Zhang, Y.-W. Tan, H. L. Störmer, P. Kim, Nature. **438**, 201 (2005).

[27] P. R. Wallace, Phys. Rev. **71**, 622 (1947).

[28] G. Semenoff, Phys. Rev. Lett. **53**, 2449 (1984).

[29] Y. Zheng, T. Ando, Phys. Rev. B **65**, 245420 (2002).

[30] V. P. Gusynin, S. G. Sharapov, Phys. Rev. Lett. **95**, 146801 (2005).

[31] V. P. Gusynin, S. G. Sharapov, Phys. Rev. B **73**, 245411 (2006).

[32] N. M. R. Peres, F. Guinea, A. H. Castro Neto, Phys. Rev. B **73**, 125411 (2006).

[33] M. V. Berry, Proc. R. Soc. London A **392**, 45 (1984).

[34] P. Carmier, D. Ullmo Phys. Rev. B **77**, 245413 (2008).

[35] V. P. Gusynin, S. G. Sharapov, J. P. Carbotte International Journal of Modern Physics B **21**, 4611 (2007).

[36] D. S. Novikov, Phys. Rev. B **76**, 245435 (2007), arXiv:0706.1391[cond-mat.mes-hall].

[37] J. W. McClure, Phys. Rev. **104**, 666 (1956).

[38] V. B. Berestetskii, E. M. Lifshitz, L. P. Pitaevskii Quantum Electrodynamics (Nauka, Moskow, 1989).

[39] O.V. Gamayun, E.V. Gorbar, V.P. Gusynin, Phys. Rev. B **80**, 165429, (2009).